Gene expression pattern of Creld2 in the fetal and postnatal kidneys of Dab1-/- mice

Đurđević, Nikolina

Master's thesis / Diplomski rad

2021

Degree Grantor / Ustanova koja je dodijelila akademski / stručni stupanj: **University of Split, School of Medicine / Sveučilište u Splitu, Medicinski fakultet**

Permanent link / Trajna poveznica: https://urn.nsk.hr/urn:nbn:hr:171:723391

Rights / Prava: In copyright / Zaštićeno autorskim pravom.

Download date / Datum preuzimanja: **2024-03-28**

SVEUČILIŠTE U SPLITU
MEDICINSKI FAKULTET
UNIVERSITAS STUDIORUM SPALATENSIS
FACULTAS MEDICA

Repository / Repozitorij:

MEFST Repository

zir.nsk.hr

UNIVERSITY OF SPLIT

dabar
DIGITALNI AKADEMSKI ARHIVI I REPOZITORIJI

UNIVERSITY OF SPLIT
SCHOOL OF MEDICINE

NIKOLINA ĐURĐEVIĆ

GENE EXPRESSION PATTERN OF CRELD2 IN THE FETAL AND POSTNATAL KIDNEYS OF DAB 1$^{-/-}$ MICE

DIPLOMA THESIS

Academic year:
2020/2021

Mentor:
Prof. Katarina Vukojević, MD, PhD, MSc

Split, July 2021

TABLE OF CONTENTS

1. INTRODUCTION 1

1.1 Embryogenesis of the kidney 2

1.1.1 Kidney systems 2

1.1.2. Collecting system 2

1.1.3. Nephrons 3

1.2. Anatomy and histology of the kidney 3

1.2.1. Renal corpuscle and blood filtration 4

1.2.2. Proximal convoluted tubule 5

1.2.3. Loop of Henle 7

1.2.4. Distal convoluted tubule and juxtaglomerular apparatus 8

1.2.5 Collecting ducts 9

1.3. CRELD2 9

1.3.1 CRELD2 in the kidney 10

1.3.2 CRELD2 in different signaling pathways 12

1.3.2.1 CRELD2 in the ER stress-response pathway 12

1.3.2.2 CRELD2 in the noncanonical WNT signaling pathway 13

1.4. Disabled-1 protein, *reeler* and *yotari* mice 13

1.4.1. The REELIN-DAB1 signaling pathway in neural tissue 14

1.4.2. DAB1 in the kidney 15

2. OBJECTIVES 16

3. MATERIALS AND METHODS 17

3.1. Ethics 18

3.2. Experimental animals 18

3.3. Tissue collection and immunohistochemistry 18

3.4. Statistics 19

4. RESULTS 20

5. DISCUSSION 28

6. CONCLUSIONS 32

7. REFERENCES 34

8. SUMMARY 38

9. CROATIAN SUMMARY 40

10. CURRICULUM VITAE 42

ACKNOWLEDGEMENT

I would like to express immeasurable appreciation and deep gratitude to my mentor Prof. Katarina Vukojević, MD, PhD, MSc, who gave me the opportunity to do my research thesis and whose invaluable guidance and kind supervision has shaped the present work as it is shown.

I would also like to extend my sincere thanks to Mirela Lozić, for assisting me with the laboratory and microscopy work required for this thesis.

I owe a deep sense of gratitude to my close friend Andrea Balić, for her true friendship over the past six years, for introducing me to her good-hearted grandparents, Nediljka Balić and Andrija Balić and their love, for making me feel at home. I will never forget these days.

Lastly, but definitely not the last, I am greatly indebted to my family. My father; Zoran Đurđević; mother Zdenka Đurđević; sister Tena Đurđević; plus, all my extended family and closest friends for supporting me from day one of my Medical School days, till the last one, without their unconditional love, sacrifices and constant encouragement, the successful completion of my studies could not have been accomplished.

LIST OF ABBREVIATIONS

PCT – Proximal convoluted tubule

GFR – Glomerular filtration rate

TAL – Thick ascending limb

DCT – Distal convoluted tubule

JGA – Juxtaglomerular apparatus

ACE – Angiotensin – converting enzyme

ADH – Antidiuretic hormone

CRELD2 – Cysteine-rich with EGF-like domains

ERSE – ER stress responsible element

ATF6 – Activating transcription factor 6

NF-Y – Nuclear transcription factor Y

BiP – Binding immunoglobulin protein

GRP78 – Glucose-regulated protein 78

MANF – Mesencephalic astrocyte-derived neurotrophic factor

ER – Endoplasmic reticulum

CAKUT – Congenital anomalies of the kidney and urinary tract

UMOD – Uromodulin

ADTKD – Autosomal dominant tubulointerstitial kidney disease

UPR – Unfolded protein response

PERK – Protein kinase R–like endoplasmic reticulum kinase

IRE1 – Inositol-requiring protein 1

MAPK – Mitogen-activated protein kinase

WNT – Wingless-related integration site

PCP – Planar cell polarity

mdab1 – Mouse disabled-1

Dab – disabled gene

DAB1 – Disabled-1 protein

PGK-neo cassette – Phosphoglycerate kinase neocassette

PI-PTB – Phosphotyrosine binding domain

PBS – Phosphate buffer saline

PFA – Paraformaldehyde

DAPI – 4',6-diamidino-2-phenylindole

1. INTRODUCTION

1.1 Embryogenesis of the kidney

1.1.1 Kidney systems

Three kidney systems are formed during the embryonic life in a rostral-to-caudal sequence within the nephrogenic cord: the pronephros, mesonephros, and the metanephros (1).

The pronephros develops at the beginning of the fourth week but has no functional role. It is composed of 7 to 10 cell groups that are located in the cervical region of the developing embryo. These cell clusters form nephrotomes, rudimentary excretory units, that regress before more caudal ones develop. The pronephros disappears already by the end of the fourth week (2).

The mesonephros is derived from mesoderm, this develops early in the fourth week, but it is situated more caudally than the pronephros, in the thoracolumbar region. The first appearing excretory tubules form an S-shaped loop and together with surrounding capillaries they form a glomerulus. Tubules around the glomerulus form the Bowman's capsule. The glomerulus and the Bowman's capsule together constitute a renal corpuscle. Laterally, the tubules enter the mesonephric or Wolffian duct, a longitudinal collecting duct. In the middle of the second month, the mesonephros presents as two large ovoid organs bilaterally. Since the gonad develops medially to the mesonephros, a urogenital ridge appears between the two structures. Finally, the mesonephros degenerates by the end of the second month, but in males some of the caudal tubules and the Wolffian duct persist to take part in the formation of the genital system (2).

The metanephros develops in the fifth week and forms the definitive kidney. Its excretory units are derived from metanephric mesenchyme, whereas the collecting system develops from the ureteric bud (2).

1.1.2. Collecting system

The collecting system of the definitive kidney includes 1 to 3 million collecting tubules approximately, the renal pelvis with its major and minor calyces, and the ureter. These structures develop from a protrusion of the mesonephric duct, just close to its entrance of the cloaca, known as the ureteric bud. A cap formed of metanephric mesoderm (blastema) forms

around the ureteric bud as it penetrates the metanephric tissue. During the sixth week, the bud widens and forms the renal pelvis and the cranial and caudal lobes of the kidney. Separation of the bud into cranial and caudal portions forms the major calyces. Two new collecting tubules develop from each calyx as it protrudes further into the metanephric mesoderm. Each new outgrowth continues to subdivide until at least 12 generations of tubules have formed. The minor calyces of the renal pelvis develop as the collecting tubules of the second generation enlarge and absorb those of the third and fourth generations, whereas the formation of the renal pyramid requires the tubules of the fifth and successive generations to elongate and converge on the previously formed minor calyx. The branching cascade continues until week 32 when one to three million collecting tubules have formed (1,2)

1.1.3. Nephrons

The excretory unit of the kidney is known as the nephron which includes the tubules, together with their glomeruli. At birth, there are approximately 1 million nephrons in each kidney (2).

The distal end of each collecting tubule is surrounded by a metanephric tissue cap, the cells of which form small renal vesicles that develop into S-shaped tubules. The free end of each tubule is invaded by capillaries, that differentiate into glomeruli. The proximal end of the tubule is indented by a glomerulus and forms the Bowman's capsule, distally the tubule joins one of the collecting tubules. This allows the future flow of urine from the glomerulus into the collecting ducts. The proximal convoluted tubule, loop of Henle and distal convoluted tubule are different parts of the nephron, which are formed by continuous lengthening of the tubules (2). The metanephros becomes functional at week eleven, but nephrogenesis is not complete until week thirty-two (1).

1.2. Anatomy and histology of the kidney

During early nephrogenesis, the two kidneys lie close to each other in the sacral region of the embryo. However, between weeks six to nine, the kidneys separate and ascend to their final position in the lumbar region (1). The kidney is a bean-shaped structure that has a convex lateral surface and a concave medial border, the hilum, where the ureter exits, the nerves enter, and the lymph vessels with the renal artery and veins enter and exit. The upper dilated end of

the ureter, called the renal pelvis, divides into two to three major calyces, that further branch into several minor calyces. Each kidney consists of an inner medulla and an outer cortex. The medulla is composed of 8-12 renal pyramids, which are separated by medullary extensions of the cortex, the renal columns. Urine that is formed by the tubules in the pyramids flows from the tip of pyramid, called the renal papilla, into the minor calyx (3).

The nephron is the functional unit of the kidney that removes metabolic waste products and excess water and electrolytes from the blood. In each kidney there are approximately 1 million nephrons. The nephron is composed of several structures: the renal corpuscle, the proximal tubule, the loop of Henle, which is situated in the medulla with its thin descending and thin ascending limb, the thick ascending limb, the distal tubule, and the connecting tubule, which combines from several nephrons to form the collecting tubules, that merge into the collecting ducts. Based on their location in the kidney, nephrons are divided into cortical nephrons and juxtamedullary nephrons, the latter of which have long loops of Henle and are situated near the medulla (3).

1.2.1. Renal corpuscle and blood filtration

The renal corpuscle is composed of a mass of capillaries, called the glomerulus, which is surrounded by a glomerular (Bowman) capsule. The Bowman capsule has two epithelial layers: the internal visceral layer that consists of complex epithelial cells called podocytes, that envelop the glomerular capillaries, and the outer parietal layer that forms the surface of the capsule and consists of a simple squamous epithelium, that is externally supported by a basal lamina. Blood that is filtered through the capillary wall and visceral layer enters the capsular, or urinary space that lies between the visceral and parietal layers. The renal corpuscle consists of a tubular pole, where the proximal convoluted tubule (PCT) begins, and a vascular pole, where the afferent arteriole enters and the efferent arteriole leaves the glomerulus. At the tubular pole, the proximal convoluted tubule is composed of simple cuboidal epithelium (3).

Primary processes extend from the podocytes of the renal corpuscle and give rise to secondary processes, called pedicles, and together they surround the glomerular capillaries. Between the pedicles are 25-30 nm wide filtration slit pores. Slit diaphragms are specialized tight junctions that bridge the slit pores and are composed of nephrins, other proteins, proteoglycans and glycoproteins. These proteins project from the cell membrane on each side

of the filtration slit and interact with each other to form openings within the slit diaphragm, with a negatively charged surface (3).

The thick glomerular basement membrane (300-360 nm) lies between the highly fenestrated endothelial cells of the glomerular capillary and the covering podocytes. The glomerular basement membrane, together with the endothelial cells of the glomerular capillaries and the podocytes forms the filtration barrier, that separates the blood from the capsular space. The meshwork of proteoglycans and type IV collagen in the basement membrane limits the passage of proteins larger than 70kDa. Smaller proteins that pass through are degraded and their amino acids reabsorbed in the proximal tubule. Filtration of organic anions is restricted by the presence of negatively charged glycosaminoglycans in the basement membrane (3).

One fifth of the blood plasma that enters a glomerulus is filtered into the urinary space. The glomerular filtrate is similar to plasma, except that it restricts the passage of macromolecules, and therefore only contains a small amount of proteins. Movement of plasma across the glomerular capillaries is favored by the high hydrostatic pressure in the arterioles that supply the glomerulus. Neural and hormonal inputs regulate the degree of constriction in the arterioles, and therefore the gomerular filtration rate. The total amount of circulating plasma averages 3 L, and the glomerular filtration rate (GFR) is estimated to be 125 mL/min or 180L/d, meaning that the kidneys filter the entire blood volume 60 times per day, but only 20% of the blood plasma entering the glomerulus is filtered into the capsular space (3).

The renal corpuscle contains mesanglial cells in addition to the glomerular capillary endothelial cells and podocytes. Mesanglial produce components of an external lamina, and together with their surrounding matrix they form the mesangium, which lies between capillaries that lack podocytes. The mesangium can contract to help maintain an optimal filtration rate and it secretes the factors required for the immune defense in the glomerulus (3).

1.2.2. Proximal convoluted tubule

The cells of the nephron tubule and collecting system reabsorb water and electrolytes, but specific activities are restricted to specialized tubular regions.

Most of the kidney cortex is filled with simple cuboidal epithelium lining the PCT, that is continuous with the squamous epithelium of the capsule's parietal layer at the tubular pole of the renal corpuscle. All the organic nutrients, such as glucose, amino acids and vitamins, as well as more than half of the water and electrolytes, that is filtered at the glomerulus are reabsorbed in the PCT. These molecules are transferred across the tubular wall and reenter the circulation through uptake into the peritubular capillaries (3).

Ion pumps, ion channels, enzymes and transporters all mediate the transcellular reabsorption of molecules through active and passive mechanisms. Leaky apical tight junctions allow the passive movement of water and certain solutes between the cells by paracellular transport along osmotic gradients (3).

Small proteins that passed the filtration barrier are degraded by peptidases on the luminal surface or reabsorbed by receptor-mediated endocytosis and degraded in the cuboidal cells, after which the aminoacids are released at the basolateral cell membrane to be taken up by capillaries (3).

Organic anions and cations that normally cannot be filtered, because of the polyanions in the filter or binding to plasma proteins, may still be secreted into the filtrate as they are released into the peritubular capillaries and absorbed by the tubular cells. Many antibiotics and other drugs are removed from the circulation by tubular secretion, which is a key mechanism of drug clearance (3).

The cells of the PCT are relatively large, so that a transverse section of the PCT typically contains only three to five nuclei, which are centrally located. The cellular cytoplasm is acidophilic because of abundant mitochondria, which are required for the ATP supply in active ion transports. Reabsorption is facilitated by the apically located brush border formed by many microvilli, which can give the lumens a fuzz-filled appearance in routine histologic preparations, when disorganized. The sparse surrounding connective tissue interstitium contains abundant peritubular capillaries (3).

Ultrastructural visualization of the cytoplasm reveals vesicles close to the apical brush border, indicating active endocytosis and pinocytosis. These vesicles contain lysosomes that degrade the reabsorbed proteins into amino acids to be released back into the circulation. The

lateral border of PCT cells shows interdigitations with neighboring cells and the basal membrane has long membrane invaginations. Both, the basolateral and the apical membrane contain transmembrane proteins that mediate tubular secretion and reabsorption. In addition, the hydroxylation of vitamin D is performed by the cells of the PCT, and fibroblasts in the cortical interstitium near PCTs produce erythropoietin, a growth factor secreted in response to cellular hypoxia that stimulates the production of red blood cells (3).

1.2.3. Loop of Henle

With the PCT tubule located in the cortex, the shorter proximal straight tubule is the continuation of the PCT in the medulla and continues as the loop of Henle. This U-shaped tubule is composed of simple squamous epithelium and is divided into a thin descending limb and a thin ascending limb. The thin limbs of the loop have a diameter of about 30 μm which is narrow, compared to the straight proximal tubular diameter of 60 μm. The thin loops of Henle have a primarily passive role in transport, as is indicated by only few organelles in the cells. The lumen of the tubule is prominent (3).

The thin ascending limb continues as the thick ascending limb (TAL), which is composed of simple cuboidal epithelium containing many mitochondria again. The thick part of the loop is situated in the outer medulla and extends as far as the macula densa, close to the glomerulus. The function of the TAL is the active transport of sodium and chloride ions out of the tubule against a concentration gradient into the medullary interstitium. In response, water is transported passively across the thin descending loop into the hyperosmotic medullary interstitium, concentrating the filtrate. The thin ascending limb is impermeable to water but reabsorbs sodium chloride. This descending and then immediately ascending flow of the filtrate in the two parallel thin limbs is known as the countercurrent flow, that establishes an osmolar gradient in the medullary interstitium. This effect is multiplied in the deeper medulla. Compared to blood, the interstitial osmolarity at the pyramidal tip is about four times higher. Vasa recta help to maintain the hyperosmotic interstitium by the countercurrent blood flow in their ascending and descending loops, and therefore play an important role in the countercurrent multiplier system together with the loops of Henle (3).

1.2.4. Distal convoluted tubule and juxtaglomerular apparatus

Situated in the cortex, the distal convoluted tubule (DCT) is the continuation of the ascending limb of the nephron. The DCT is lined by simple cuboidal cells and is distinguished from the PCT in the cortex by its smaller cell size and empty lumen from a missing brush border, because it is less involved in tubular reabsorption. In addition, more nuclei are seen in transverse sections of distal tubules and the cytoplasm is less acidophilic, because the cells are flatter and have fewer mitochondria compared to the cells of the PCT. Aldosterone, secreted by the adrenal glands is the key regulator of sodium absorption in the DCT (3).

The macula densa is the initial straight part of the distal tubule that is situated near the arterioles of the vascular pole of the parent renal corpuscle. The cells are more columnar and densely packed. The macular densa is part of the juxtaglomerular apparatus (JGA), a specialized sensory structure that regulates the glomerular blood flow through feedback mechanisms, to keep the rate of glomerular filtration relatively constant. Typical for the cells of the macula densa are the apically situated nuclei, basal Golgi complexes, and a complex system of transporters and ion channels. Located closely to the macula densa are the smooth muscle cells of the afferent arteriole, which are modified as juxtaglomerular granular cells and have a secretory phenotype that includes rough ER, Golgi complexes, more rounded nuclei and zymogen granules containing renin (3).

The autoregulatory mechanisms of the GFR are under the control of the JGA and include the following activities. High arterial pressure increases the glomerular capillary blood pressure, which in turn increases the GFR. In response to a higher GFR, the luminal concentrations of sodium and chloride in the TAL are increased, which is sensed by the cells of the macula densa and causes these cells to release vasoactive compounds such as ATP and adenosine. Triggered by these vasoactive substances, the afferent arteriole contracts to lower the glomerular pressure and therefore to lower the GFR (3).

A decrease in arterial pressure is sensed by local barorecptors in the afferent arteriole, which stimulates the JGA to release renin, an aspartyl protease, into the blood. Renin cleaves angiotensinogen into angiotensin I that is further converted to angiotensin II by angiotensin-converting enzyme (ACE) on lung capillary endothelium. As a potent vasocontrictor, angiotensin II directly raises the systemic blood pressure and stimulates the adrenal glands to

secrete aldosterone. Stimulated by aldosterone, the cells in the DCT and connecting tubule promote sodium and water reabsorption in order to raise the circulating blood volume, and therefore to increase the blood pressure (3).

1.2.5 Collecting ducts

The connecting tubule is the last part of a nephron and several join in the cortical medullary rays to form collecting ducts of simple cuboidal epithelium, which merge further as larger collecting ducts of Bellini. These larger ducts are lined by simple columnar cells and run to the apex of the medullary pyramids, where they merge as papillary duct that empties urine into the minor calyx. The interstitium around the medullary collecting ducts has a very high interstitial osmolarity. The pale-staining columnar principal cells make up most of the collecting ducts. These cells have sparse microvilli, few organelles and distinct cell boundaries. Ultrastructurally basal membrane infoldings can be seen that are consistent with their role in ion transport, and a primary cilium is located among the microvilli. Principal cells express aquaporins, specific protein channels for water molecules, that are regulated by anti-diuretic hormone (ADH). In response to dehydration the pituitary gland releases ADH, which increases the permeability to water in the collecting tubules. The binding of ADH to receptors on the basolateral membrane stimulates the movement and insertion of aquaporin-containing vesicles into the apical (luminal) membranes to facilitate the water movement through the cells. The hyperosmolar interstitium further concentrates the filtrate by drawing water passively from the collecting ducts (3).

The second type of cells that occur in collecting ducts are intercalated cells, which stain darker, contain more mitochondria, and have projecting apical folds. Intercalated cells regulate the acid-base homeostasis by secreting either H+ or HCO3- (3).

1.3. CRELD2

The Cysteine-rich with EGF-like domains (CRELD) family of proteins comprises the members CRELD1 and CRELD2. As mutated CRELD1 is associated with cardiac atrioventricular septal defects, the *CRELD1* gene is also known as the *AVSD2* gene. *CRELD1* and *CRELD2* are both highly conserved genes with orthologues and homologues found in different species (4).

CRELD2 is a ~50kDa secretory glycoprotein that is localized in the endoplasmic reticulum (ER) and Golgi apparatus and is highly activated under ER stress. It has been shown that modifications on its C-terminal end, which contains four aminoacids (REDL), enhance its secretion from the ER (5, 6, 7). It is suggested that CRELD2 has important roles both in the ER-Golgi apparatus and in the extracellular space during normal and pathophysiological conditions (5). Mapping of human *CRELD2* by FISH localizes the gene to locus 22q13.33 (4, 8). The ortholog gene in mice is located on chromosome 15; 15 E3 (9). The *Creld2* gene in mice correlates with the *CRELD2α* gene in humans (7). Alternative splicing of *CRELD2* results in five known CRELD2 isoforms which function has yet to be fully understood (4). It is predicted that CRELD2 isoforms are secreted freely into the extracellular space, except for CRELD2β which is localized to the ER and found to regulate the α4β2 nicotinic acetylcholine receptor expression in the nervous system (10). In contrast, the major CRELD1 isoform CRELD1α is found to be a cell adhesion molecule since it contains multiple EGF domains (4).

The mouse *Creld2* promoter contains the genomic sequence of a typical ER stress responsible element (ERSE), which is well conserved among different species (7). The ER stress master regulator activating transcription factor 6 (ATF6) and nuclear transcription factor Y (NF-Y) positively regulate the transcription of the *Creld2* gene through the ERSE at the proximal region of the mouse *Creld2* promoter (7). Binding immunoglobulin protein (BiP), also known as glucose-regulated protein 78 (GRP78), and mesencephalic astrocyte-derived neurotrophic factor (MANF) increase the secretion of CRELD2 through interaction with ATF6 (5, 11, 12). This suggests that CRELD2 could be an important regulator of cellular homeostasis from responses to unfolded or misfolded proteins and might act as a mediator in the development of different ER stress-associated diseases (7).

CRELD2 expression is found to be the highest in adult endocrine tissues, but CRELD1 and CRELD2 are ubiquitously expressed in fetal and adult tissues (4). And still, to date a full understanding of the CRELD2 protein expression is missing (12).

1.3.1 CRELD2 in the kidney

The pathogenesis of various glomerular and tubular kidney diseases is based on signaling pathways related to endoplasmic reticulum (ER) stress (13). The ER is the site of protein folding and modification of newly synthesized transmembrane and secretory proteins,

but in some pathophysiological conditions ER function can be disrupted by accumulation of unfolded or misfolded proteins, which is referred to as ER stress (14, 15). Recent studies have identified CRELD2 as a urinary biomarker for ER stress-mediated kidney diseases (13, 6).

Creld2 was first identified to be an ER stress-inducible protein by studying the gene expression of mouse neuro2α cells treated with the ER stress-inducing agent thapsigargin through microarray analysis. Two other ER stress inducers, tunicamycin and brefeldin A also increased the expression of Creld2 mRNA (10). Further, urinary Creld2 was found to be a sensitive biomarker for detecting ER stress in podocytes and renal tubular cells in mouse models of podocyte ER stress-induced nephrotic syndrome and tunicamycin- or ischemia-reperfusion-induced acute kidney injury, respectively (13).

A recent study investigated the genetic expression pattern of CRELD2 in human fetal and postnatal kidneys and found CRELD2 to have an important role in genitourinary tract development as well as for the maintenance of kidney homeostasis. It was further suggested that mutations in CRELD2 might lead to the development of congenital anomalies of the kidney and urinary tract (CAKUT) (16).

Mutations in the uromodulin (UMOD) gene are proven to be a genetical cause for the induction of ER stress in cells of the TAL. Autosomal dominant tubulointerstitial kidney disease (ADTKD) is caused by UMOD mutations and is a prototypical tubular ER stress disease that leads to progressive loss of kidney function. Urinary CRELD2 was found to be a sensitive ER stress biomarker for ADTKD-UMOD and therefore measurement of CRELD2 in the urine could be useful to monitor the response to new therapies for this monogenic form of renal fibrosis (13).

There is a strong association between the detection of urinary CRELD2 within postoperative 6 hours after pediatric cardiac surgery and severe postoperative acute kidney injury (13). Overall, CRELD2 could be a potentially novel ER stress biomarker for the early diagnosis of rare kidney diseases, when a kidney biopsy is not yet clinically indicated and as such can help accelerate therapeutic intervention (13).

In addition, high expressions of CRELD2 in renal cell carcinoma were found to be associated with poor prognosis (17). Interestingly, CRELD1 is found to be one of the candidate

cystogenic proteins that induce cyst formation in autosomal dominant polycystic kidney disease (18).

1.3.2 CRELD2 in different signaling pathways

1.3.2.1 CRELD2 in the ER stress-response pathway

In response to ER stress, signal transduction pathways collectively termed the unfolded protein response (UPR) are activated. The three identified ER stress sensors are protein kinase R–like endoplasmic reticulum kinase (PERK), inositol-requiring protein 1 (IRE1) and ATF6 that regulate the expression of ER stress-inducible genes. The signaling cascade either protects the cell and controls cell survival or it eventually leads to apoptosis in the affected organ (14, 15). Under normal conditions, binding of BiP/GRP78 to the three ER stress sensors inactivates the ER stress response (12). The ER stress response is activated when BiP/GRP78 dissociates from the ER stress sensors and adheres to the misfolded proteins (14).

ATF6 belongs to the basic-leucine-zipper family of transcription factors (19,20) and is found to positively regulate the expression of CRELD2 under ER stress conditions (10, 12). It is a 90 kDa glycoprotein located in the ER membrane (12). Under ER stress ATF6 translocates to the Golgi apparatus and is cleaved by site-1 and site-2 proteases (14). This translocation requires a dissociation step from its inhibitory regulator BiP/GRP78 (21,22). The resulting N-terminal 50 kDa fragment (p50 ATF6) is an active transcription factor that regulates the UPR gene expression in the nucleus (14). In response, UPR-targeted genes including the ER chaperone CRELD2 will be expressed to assist in restoring normal cellular function (14) and maintain cellular homeostasis upon ER stress (20). If the UPR is unable to maintain the ER proteostasis, ER stress-mediated apoptosis occurs (14).

Interestingly, ATF6 was reported to have a role in kidney disease. Overexpression of the active form of ATF6 causes excessive lipid droplets formation in human proximal kidney tubules, that leads to upregulation of renal pro-fibrotic genes (23). Since CRELD2 is regulated by ATF6 in ER stress-response pathways, there might be a link between ATF6 overexpression and CRELD2-mediated kidney disease.

In the mammary tumour epithelium CRELD2 was found to have a role in the progression of breast cancer by acting downstream in the Rho-associated kinase (ROCK)-

PERK-ATF4 signaling cascade (24). Furthermore, in prostate cancer CRELD2 was reported to be one of the novel androgen receptor target genes, that mediate the receptor's roles in disease progression (25). Therefore, the identification of CRELD2-dependent signaling pathways further might have implications in cancer therapy.

1.3.2.2 CRELD2 in the noncanonical WNT signaling pathway

CRELD2 is proven to promote the differentiation and maturation of skeletal cells by regulating the noncanonical p38 MAPK WNT signaling pathway. CRELD2 promotes the expression of low-density lipoprotein receptor-related protein 1 (LRP1) at the cell membrane, which binds to TGFβ-1 to further regulate WNT4 expression in chondrocytes (26).

WNT signaling is classified into the canonical (β-catenin-dependent) or noncanonical (β-catenin-independent) pathway and the latter includes WNT/planar cell polarity (PCP) and WNT/Ca^{+2} signaling routes. Furthermore, the canonical and the noncanonical WNT/PCP pathway are found to have an outmost importance in early kidney development, such as in ureteric bud formation and nephrongenesis, and are implicated in various kidney disorders (27).

The finding that CRELD2 regulates noncanonical WNT signaling in chondrocytes might implicate a not yet identified role of CRELD2 in the noncanonical signaling pathway in the kidney.

1.4. Disabled-1 protein, *reeler* and *yotari* mice

Mammalian neurodevelopment is based on the radial migration of embryonic neurons from the neuroectoderm to defined locations to form distinct cell layers in the brain (28). *Mouse disabled-1* (*mdab1*) is a mouse homolog of the Drosophila *disabled* (*Dab*) gene, that encodes a cytoplasmic adaptor protein that has an important role in neuronal positioning during brain development (29, 30). Homozygous $Dab1^{-/-}$ *yotari* mice have an autosomal recessive mutation of *Dab1* and express a phenotype that is very similar to Reelin-deficient mice (31). Originally, *yotari* mice arose unintentionally in the descendants of a male chimeric mouse, that was thought to produce a knockout mouse of an unrelated gene (32,33). In *yotari* mice the mutated *Dab1* gene is partially replaced with a long interspersed nuclear element (L1) fragment and therefore, an aberrant fragment of the Dab1 protein (p64/60) is expressed in the yotari brain (33). Compared to the wild-type Dab1 protein, the fragmented p64/60 form is not

phosphorylated by Fyn kinase and is found predominantly in the nucleus, whereas Dab1 is a cytoplasmic protein (33).

In *reeler* mice the mutated gene is *reelin* (32), which encodes an extracellular signaling molecule (REELIN) in Cajal-Retzius cells in the forebrain and granule neurons in the cerebellum, that coordinates the ordered neuronal alignment during mammalian neurodevelopment (29,34,35). Although the mutations in *reeler* and *yotari* mice are different, both mutations are on the same signaling pathway, which explains some of the common behavioral and pathological phenotypes in these two mutants (32). The phenotype consists of an unstable gait and intermittent tremor (32) with hypoplasia of the cerebellum and other histological abnormalities of the hippocampus and cerebral cortex from neuronal misplacement (28,29,31). And still, one important discrepancy exists between *reeler* and *yotari* mice: *reeler* mice live into adulthood, whereas *yotari* mice die before reaching maturity and therefore cannot reproduce (32,33). Somehow, *yotari* mice are more severely affected by their mutation than are *reeler* mice, which in future could be a new field of investigation (32,33).

1.4.1. The REELIN-DAB1 signaling pathway in neural tissue

Dab1 is a phosphoprotein that acts as an intracellular adaptor in protein kinase pathways and acts downstream of Reelin during neurodevelopment, the finding of which was made through studies conducted on the *yotari* mouse model (29,33). Today we know that DAB1 tyrosine phosphorylation is also required for correct migration of sympathetic preganglionic neurons in the spinal cord, and therefore the REELIN-DAB1 signaling pathway has an important role during the development of the central nervous system in general (33,36).

DAB1 binds to the intracellular part of REELIN receptors, apolipoprotein E receptor 2 (ApoER2) and the very low-density lipoprotein receptor (VLDLR) (33). Through extracellular binding of REELIN to its receptors, DAB1 is phosphorylated on its tyrosine residues by Src family tyrosine kinases and subsequently activates a variety of SH2 domain-containing proteins. This leads to the activation of multiple signaling pathways that result in correct neuronal positioning and remodeling of cytoskeleton (30,33,37).

1.4.2. DAB1 in the kidney

DAB1 is found to be highly expressed in the DCT during fetal kidney development (38). This finding could attribute DAB1 a potentially important role in tubular formation or function maintenance during the human kidney embryogenesis (38). Interestingly, a recent study conducted on *yotari* mice discovered Dab1$^{-/-}$ mice to have hypoplastic kidney tissue with podocyte foot process effacement, suggesting that mutated DAB1 seems to be involved in the development of CAKUT, while further supporting the idea that DAB1 has a role in early nephrogenesis (39). Additionally, DAB1 is shown to contribute to angiotensin II-induced podocyte apoptosis, emphasizing its possible role in kidney disease (40).

The role of CRELD2 in human kidney embryogenesis, tumor progression and skeletal malformations is currently a field of research, but until now, the expression pattern and the role of CRELD2 in kidneys of Dab1$^{-/-}$ mice has not yet been investigated.

2. OBJECTIVES

The aim of this study was to analyze the expression and localization of Creld2 in the nephrons of *yotari (Dab1*$^{-/-}$) and *wildtype (Dab1*$^{+/+}$*)* mice to further explore its suggested importance not only in mammal kidneys overall, but also the significance it may have particularly in the *yotari* mouse nephron.

Hypothesis:

Creld2 will have a significantly different expression pattern in the kidney nephrons of *yotari* and *wildtype* genotypes.

3. MATERIALS AND METHODS

3.1. Ethics

The experimental protocol was approved by the Ethics Committee of the University of Split School of Medicine and conducted according to the Croatian Animal Welfare Act.

3.2. Experimental animals

We observed two groups of pups according to their *Dab1* gene status: *yotari* ($Dab1^{-/-}$) and *wildtype* ($Dab1^{+/+}$) controls. *Yotari* mice were produced by PGK-neo cassette which resulted in target disruption of the first 47 codons of the gene coding for the protein-interlacing domain (PI-PTB). At least one mouse of each group was group-housed and raised in standard polycarbonate cages. The mice were held in a temperature-controlled (23±2°C) room with a 12-h light/dark cycle and their access to water and food was *ad libitum*.

3.3. Tissue collection and immunohistochemistry

Female pregnant mice on gestational day 13.5 and pups on the 4th and 14th postnatal day were anesthetized deeply with pentobarbital and were transcardially perfused with phosphate buffer saline (PBS, pH 7.2) and 4% paraformaldehyde (PFA) in 0.1 M PBS.

Fetuses of pregnant mice and kidneys of postnatal mice were removed and embedded in paraffin to be cut transversely into 7 µm thin sections afterwards. We prepared 4 microscopic slides consisting of 11 fetal sections, and 5 slides consisting of 7 postnatal kidney sections for each of the two yotari and wildtype mouse groups, respectively. The deparaffinization of sections in xylene was followed by rehydration in ethanol and water and treatment with heated sodium citrate buffer (pH 6.0) for 30 minutes in the Epitope Retrieval Steamer. After washing in PBS, the samples were separated with a PAP pen hydrophobic pencil. The samples were incubated with primary antibodies against CRELD2 overnight in a humidity chamber. Rabbit polyclonal *Anti-CRELD2* ((G-17); SC-86110 Santa Cruz) was diluted 1:100 in Dako REAL antibody dilutent (Dako Denmark A/S, Glostrup, Denmark), and then applied to the sections. The next day, sections were washed with PBS and incubated with secondary antibodies in the humidified chamber for one hour and washed with PBS again. Alexa Fluor 488 AffiniPure Donkey Polyclonal Anti-Rabbit IgG (Jackson IR, 711-545-152) against CRELD2 primary antibody-stained samples was used. The nuclei of the tissue samples were stained with 4’6’-diamidino-2-phenylindole (DAPI). The stained kidney sections were viewed and photographed

using an Olympus fluorescence microscope (Olympus BX51 Tokyo, Japan) equipped with a DP71 digital camera (Olympus). The final step involved the processing of the images with CellA Imaging Software for Life Sciences Microscopy (Olympus). Using Adobe Photoshop (Adobe, San Jose, CA, USA) microphotographs were processed and then analysed with ImageJ software. Different structures of the kidney were analyzed: the PCT, glomerulus and DCT in all kidney samples, in addition to the renal vesicle, ureteric bud and metanephric mesenchyme in the embryonal kidney sections (Figures 1-3). For each kidney section five non-overlapping fields were photographed at x40 objective magnification, with each field constituting one image. Analysis was performed by counting CRELD2 immunoreactive (positive), and negative cells within PCTs, glomeruli and DCTs, using ImageJ software (National Institutes of Health, Bethesda, MD USA). CRELD2 positive cells were determined by the colour staining intensity (green). Finally, the percentages of CRELD2 positive cells in the PCT, glomeruli and DCT were compared and tested for statistical significance within one mouse group, as well as between the *yotari* and *wildtype* mouse groups.

3.4. Statistics

The Kolmogorov-Smirnov test was applied to test for a normal data distribution, after which statistical analysis was performed using a Kruskal-Wallis test in GraphPad (GraphPad Software, La Jolla, CA, USA) to examine differences in the 3 kidney structures (PCT, glomeruli, and DCT) within one mouse group. Comparison of kidney structures between the *yotari* and *wildtype* group was performed using t-test. The percentage of positive cells was expressed as the mean ± standard deviation (SD). Statistical significance was set at $P<0.05$.

4. RESULTS

The expression pattern and percentage of Creld2 positive cells was analyzed in the PCT, glomeruli, and DCT of 13.5-day old embryonal kidneys, and 4 and 14 days old postnatal kidneys of Dab1$^{-/-}$ *(yotari)* and Dab1$^{+/+}$ (*wildtype)* mice. Within each of the two mouse groups, the percentages of Creld2 positive cells were compared between the PCT, glomeruli, and DCT, and tested for statistical significance ($P<0.05$). Next, the percentages of Creld2 positive cells were compared between the *yotari* and *wildtype* mouse group to be tested for statistically significant difference in expression in examined kidney structures (PCT, glomeruli and DCT). Representative images of *wildtype* and *yotari* mouse kidney samples on embryonal day 13.5 (E13.5) and postnatal day 4 (4D) and 14 (14D) respectively, are shown below (Figures 1-3).

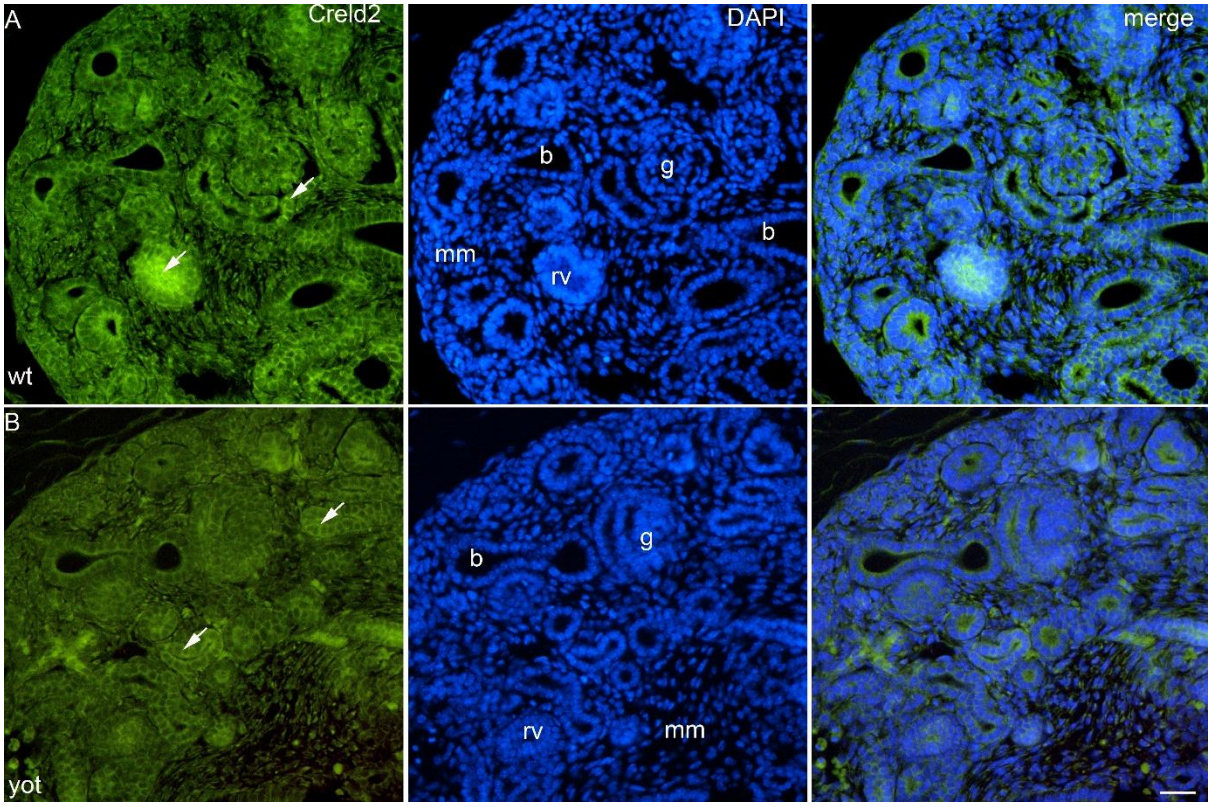

Figure 1. E13.5. Immunofluorescence staining with Creld2 antibodies (green signal, arrows) and DAPI (blue-stained nucleus) in E13.5 *wildtype* (wt) (Figure A) and *yotari* (yot) (Figure B) mouse kidney samples. Co-localization of Creld2 and DAPI nuclear stain is shown in the right column (merge). Legend: rv- renal vesicle; b- ureteric bud; mm- metanephric mesenchyme; g- glomerulus, p- proximal convoluted tubule; d- distal convoluted tubule. Scale bar 20 µm.

In the E13.5 *wildtype* kidney samples, stained with Creld2 antibodies, only the renal vesicles and glomeruli showed intermediate expressions of Creld2 (arrows) (Figure 1A). In comparison, in the *yotari* kidney samples on E13.5 there was the occasional positive cell within the renal vesicle or the glomerulus (arrows) (Figure 1B).

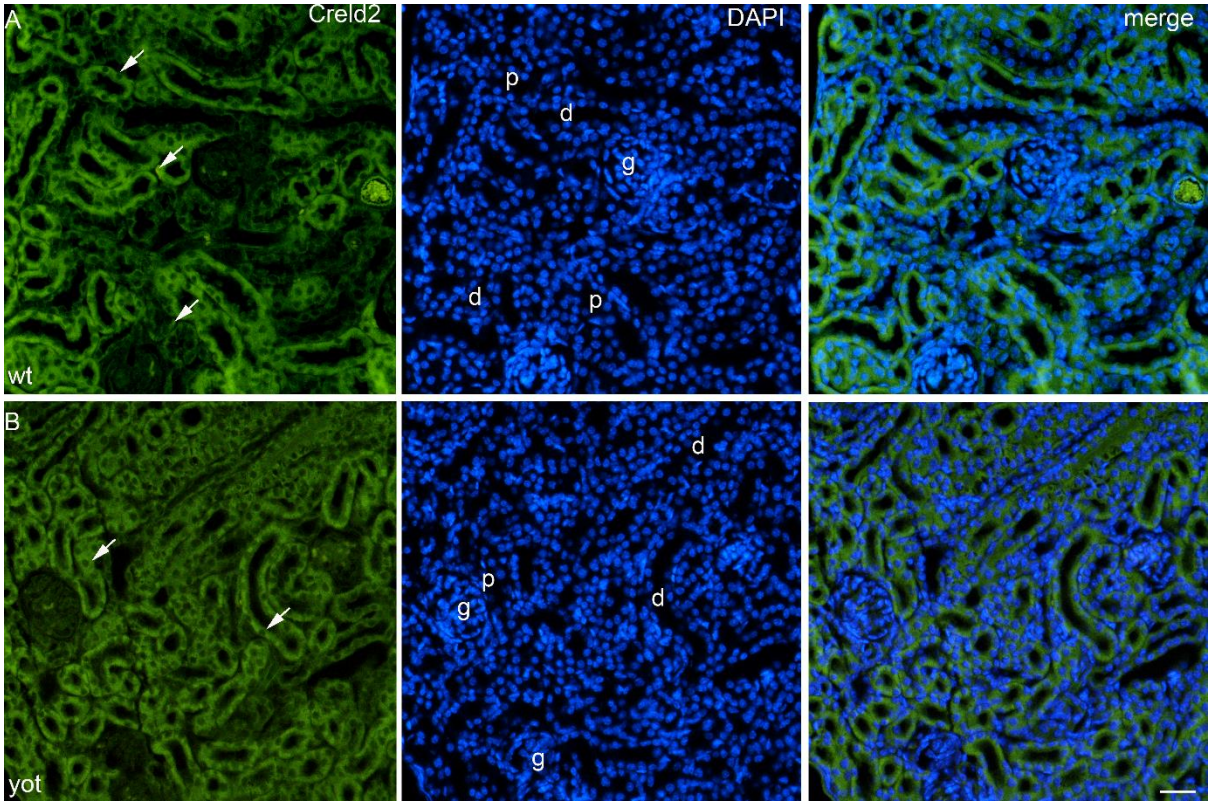

Figure 2. 4D. Immunofluorescence staining with Creld2 antibodies (green signal, arrows) and DAPI (blue-stained nucleus) in 4D *wildtype* (wt) (Figure A) and *yotari* (yot) (Figure B) mouse kidney samples. Co-localization of Creld2 and DAPI nuclear stain is shown in the right column (merge). Legend: g- glomerulus, p- proximal convoluted tubule; d- distal convoluted tubule. Scale bar 20 µm.

In the 4D *wildtype* kidney samples there was strong Creld2 expression in the cytoplasm of the PCTs (arrow) and some little expression in the DCTs (arrow) (Figure 2A). The 4D *yotari* kidney samples showed intermediate to high Creld2 expressions in the cytoplasm of the PCT (arrow). Barely any positive cells were found in the cytoplasm of the DCTs (arrow) and the glomeruli (Figure 2B).

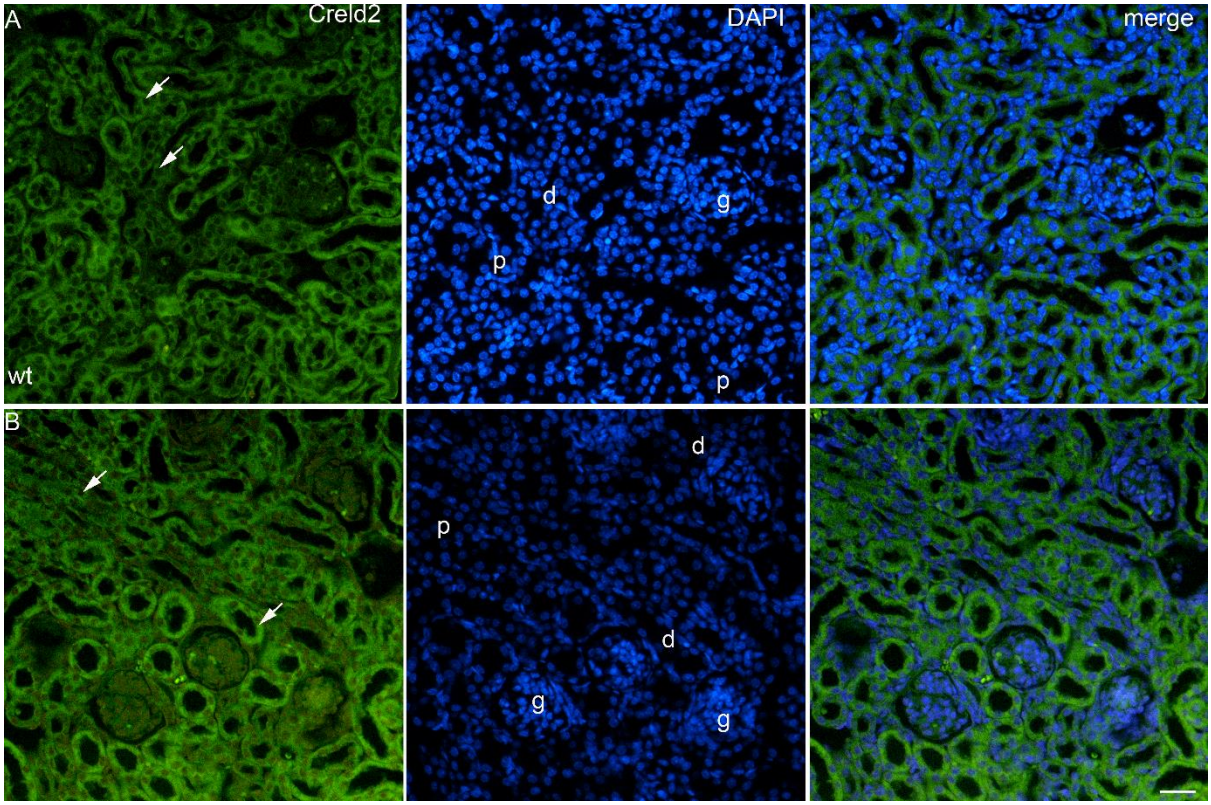

Figure 3. 14D. Immunofluorescence staining with Creld2 antibodies (green signal, arrows) and DAPI (blue-stained nucleus) in 14D *wildtype* (wt) (figure A) and *yotari* (yot) (figure B) mouse kidney samples. Co-localization of Creld2 and DAPI nuclear stain is shown in the right column (merge). Legend: g- glomerulus, p- proximal convoluted tubule; d- distal convoluted tubule. Scale bar 20 µm.

In the 14D *wildtype* kidney samples there was very strong Creld2 expression in the cytoplasm of the PCTs (arrow), and some intermediate expression in the DCTs (arrow) (Figure 3A). In the 14D *yotari* kidney samples there was strong Creld2 expression in the cytoplasm of the PCTs and little expression in the cytoplasm of the DCTs (arrow) (Figure 3B).

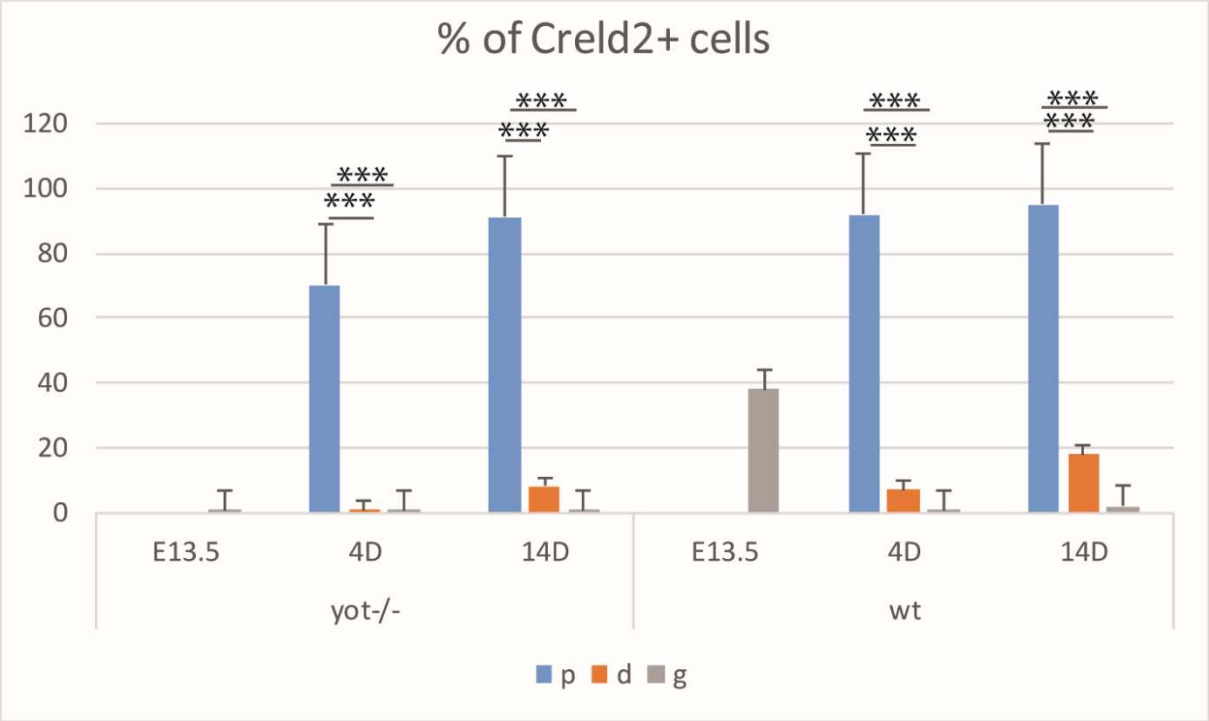

Figure 4. The distribution of percentages of Creld2 positive cells in the proximal convoluted tubules (p; blue), distal convoluted tubules (d; orange), and glomeruli (g; grey) in E13.5, 4D, and 14D *yotari* (yot-/-) and *wildtype* (wt) mouse kidneys. Data is presented as the mean ± standard deviation (SD) (vertical line). Significant differences between the p, d, and g within the *yotari* and *wildtype* nephrons are indicated by ***P<0.001 (Kolmogorov-Smirnov test for data distribution followed by a Kruskal-Wallis test).

On E13.5 glomeruli of *yotari* and *wildtype* kidneys expressed 1% and 38% of Creld2 positive cells, respectively, and the PCTs and DCTs showed no expressions neither in the *yotari* nor in the *wildtype* kidney samples (Figure 4). Within each of the two mouse groups no significant differences in prenatal Creld2 expression were found between the three assessed kidney structures (PCT, DCT and glomerulus) (Figure 4).

When comparing the percentages of positively expressed cells between the PCT, DCT, and glomerulus on postnatal day 4D, the PCTs showed significantly higher Creld2 expressions compared to the DCTs and glomeruli (P<0.001), with 70% and 92% of positively stained cells within the *yotari* and *wildtype* kidney samples, respectively (Figure 4).

The PCTs expressed even higher percentages of immunoreactive cells on postnatal day 14D, with 91% and 95% within the *yotari* and *wildtype* group, respectively (Figure 4). Compared to the much lower Creld2 expression in the DCTs and glomeruli, the PCTs in both, *yotari* and *wildtype* nephrons are proven to express significantly higher percentages of Creld2 positive cells (P<0.001) (Figure 4).

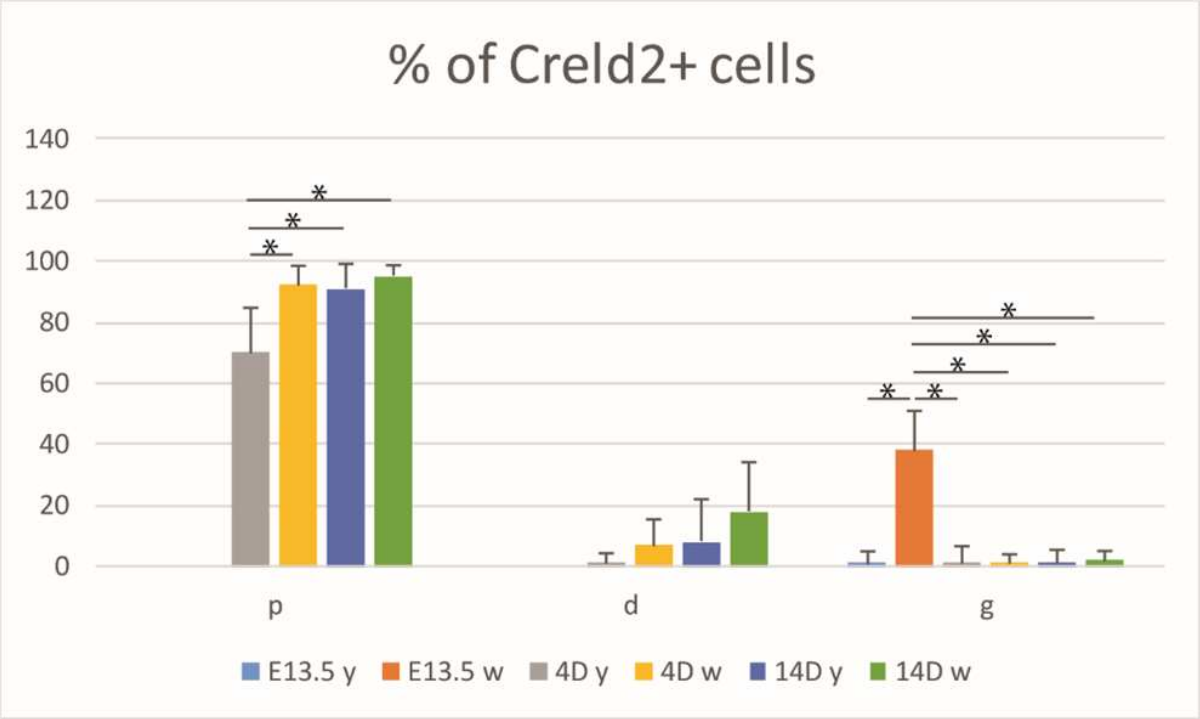

Figure 5. The distribution of percentages of Creld2 positive cells in the proximal convoluted tubule (p), distal convoluted tubule (d), and glomerulus (g) on embryonal day E13.5 and postnatal days 4D and 14D in the nephrons of *yotari* (y) and *wildtype* (w) mice. Data is presented as the mean ± standard deviation (SD) (vertical line). Significant differences in Creld2 expression between the (p), (d), and (g) of the *yotari* and *wildtype* nephrons are indicated by *P<0.05 (Kolmogorov-Smirnov-test for data distribution followed by a t-test).

When comparing the percentages of positively stained cells between the *yotari* and *wildtype* kidney samples on postnatal day 4D in the PCT, there was a statistically significant higher percentage of positive cells in the *wildtype* group (P<0.05) (Figure 5). Within the *yotari* mouse group, the PCTs showed a significantly higher percentage of Creld2 expressing cells on postnatal day 14D when compared to postnatal day 4D (P<0.05) (Figure 5).

The highest Creld2 expressions overall were found in *wildtype* PCTs on postnatal day 14D, with 95% of positively expressed cells, which showed a statistically significant higher percentage of immunoreactive cells when compared against the other mouse groups (P<0.05) (Figure 5).

There were no statistically significant differences found between the *yotari* and *wildtype* group in the DCT when comparing the percentages of Creld2 positive cells (Figure 5).

The glomeruli showed the highest percentage of Creld2-expressing cells in E13.5 *wildtype* kidney samples with 38% of positively stained cells. When comparing between the other mouse groups, glomeruli of E13.5 *wildtype* nephrons had a statistically significant higher percentage of immunoreactive cells ($P<0.05$).

5. DISCUSSION

The expression and localization of Creld2 in E13.5, 4D and 14D kidneys of *yotari* (Dab1$^{-/-}$) and *wildtype* (Dab1$^{+/+}$) mice was investigated to characterise the Creld2 expression pattern in the kidney structures.

Previous studies conducted on homozygous Dab1$^{-/-}$ *yotari* mutant mice revealed renal hypoplasia that is characteristic of a CAKUT phenotype in *yotari* mice. Additionally**,** Dab1$^{-/-}$ *yotari* mutant mice had foot process effacement implying congenital nephrotic syndrome (39). Racetin *et al* discovered that *yotari* mice do not show abberations in the structure of the PCT and DCT, therefore these structures are not affected by the mutations in the Dab1 gene (38). However, the underlying mechanism that led to CAKUT and congenital nephrotic syndrome in these mice remains unknown.

Latest studies identify the *CRELD2* gene as a CAKUT candidate gene, as mutations in CRELD2 may lead to the development of CAKUT. These findings were confirmed in human fetal and postnatal kidney tissue, by significantly high expressions of CRELD2 in the developing and mature kidneys (16). Therefore, through this research we wanted to establish the differences between the *wildtype* and *yotari* mice's Creld2 expression patterns, which may imply crosstalk between these two genes pathways.

In this study, the highest percentages of Creld2 positive cells were found in both, *yotari* and *wildtype* groups in the 14D PCTs, with statistically significant higher Creld2 expression in the *wildtype* group. Furthermore, the PCTs of 4D postnatal kidney samples also showed significantly higher Creld2 expressions in the *wildtype* nephrons when compared to the *yotari* nephrons. Interestingly, when comparing the percentages of Creld2 positive cells in the PCT, DCT and glomeruli between postnatal 14D *yotari* kidney samples and postnatal 4D *wildtype* kidneys, it is evident that these percentages are almost identical. This implicates a lack or delay of Creld2 expression in the *yotari* mouse group when compared to the healthy control group, and therefore may indicate a connection of Dab1$^{-/-}$ with the expression of Creld2. Further studies are required to establish a longer timeline after 14D, as well as molecular expression of these genes that would show more accurate quantification (qPCR and WB techniques). Lasić *et al.* investigated expressions of CRELD2 in the human prenatal and postnatal kidneys and found the highest staining intensity in the PCTs, with the highest rate in 13-week-old prenatal and 1.5year old postnatal human kidneys (16). In contrast, in this study prenatal E13.5 *yotari* and *wildtype* mouse kidneys did not show any expressions of Creld2 neither in the PCTs, nor

in the DCTs. These findings may suggest that Creld2 has no role in the embryonal development of the mouse PCT and DCT at this early stage of development. Significantly higher Creld2 expressions were found in the PCTs of 14D kidney samples when compared to the 4D PCTs in both *yotari* and *wildtype* kidney samples in our research. Therefore, we suggest that Creld2 in the mouse kidney has a more important role in tubular function than during the early development of the tubular structures.

The DCTs expressed Creld2 positive cells only in postnatal 4D and 14D kidney samples, and no statistically significant differences were found in Creld2 expression between the mouse groups. This finding is consistent with the study conducted by Racetin *et al.*, that found *yotari* mice to have no aberrations in the structure of the DCT, and therefore the Dab1$^{-/-}$ mutation seems to have no greater impact on the DCTs (39). Lasić *et al.* found expression of CRELD2 in both, fetal and postnatal human kidney samples with statistically significant differences in Creld2 expression between the checked periods. Our study did not find any Creld2 expressions in embryonal E13.5 PCTs and DCTs, which might imply differences between human and murine Creld2 expression pattern, but this cannot be said for sure, as the fetal kidney samples in Lasićs study were derived from older fetal kidney samples, and therefore these fetal periods cannot be compared.

From the three structures analyzed, only the glomeruli stained positive in the embryonic E13.5 kidney samples, with the *wildtype* group expressing significantly more Creld2 compared to the *yotari* group. Overall, the glomerulus expressed the highest percentage of Creld2 positive cells on embryonal day E13.5. Kim *et al.* identified mouse podocytes to express and secrete increased levels of Creld2 in response to ER stress (13). Lasić *et al.* further interpret the high CRELD2 expressions during the embryonal development of healthy human kidneys by speculating about possible ER stress from tissue hypoxia from high differentiation and proliferation rates (16). This may also be the reason for the relatively high percentage of Creld2-expressing cells in glomeruli of E13.5 mouse kidneys in this study. Furthermore, glomerular Creld2 expressions were shown to decrease extremely postnatally in the 4D and 14D *wildtype* kidney samples, implicating a rather more important role of Creld2 during early glomerular development, than glomerular function maintenance. In contrast, glomeruli in the *yotari* kidney samples showed constant minimal expressions of Creld2 in the embryonal and postnatal stages, therefore Creld2 expression in the glomeruli of *yotari* mice is slightly affected by the mutation in the *Dab1* gene.

Using immunofluorescence staining, Creld2 was found to be localized in the cell cytoplasm, but by only using this method, the subcellular location of Creld2 cannot be specified. Therefore, this study cannot establish an exact role of Creld2 in the mouse kidney. Oh-hashi *et al*. demonstrated a predominant localization of Creld2 in the ER and Golgi apparatus, but through modifications on its C-terminal end it is secreted into the extracellular space (5).

Overall, it was shown that Dab1$^{-/-}$ *yotari* mutant mice had lower Creld2 expressions compared to the *wildtype* mice. Postnatally Creld2 was found to have a possible role in function maintenance especially in the PCT and lesser in the DCT, whereas no Creld2 expressions were found in the PCT and DCT in embryonal kidney samples. The appearance of significantly high Creld2 expressions in the glomeruli during the fetal kidney development in the mouse confirm the potential significant role of Creld2 in the formation of kidney structure.

6. CONCLUSIONS

1. The highest percentage of Creld2 positive cells in all checked periods was found in the PCT in postnatal 14D *wildtype* kidney samples.
2. In examined and control mouse groups, the PCTs of 14D postnatal kidneys showed a significantly higher Creld2 expression when compared against the 4D postnatal kidneys. This indicates the importance of Creld2 in the later postnatal period in possible function maintenance of the PCT.
3. The PCTs of postnatal 4D and 14D *wildtype* kidney samples showed significantly higher expressions compared to the *yotari* group, which might implicate delayed Creld2 expression in *yotari* kidneys.
4. In the prenatal E13.5 *yotari* and *wildtype* kidney samples, immunoreactive cells were exclusively detectable in the glomeruli, with the *wildtype* group showing significantly higher Creld2 expressions during early glomerular development. Therefore, Creld2 expression in the glomeruli of *yotari* mice is slightly affected by the Dab1$^{-/-}$ mutation.
5. The DCTs expressed Creld2 positive cells only in postnatal 4D and 14D kidney samples, and no statistically significant difference in Creld2 expression being found between the mouse groups, therefore the Dab1$^{-/-}$ mutation seems to have no greater impact on the DCTs.
6. Prenatally the PCT and DCT of *yotari* and control mouse groups did not express any Creld2 positive cells, indicating that Creld2 has no role in the embryonal development of the mouse PCT and DCT at E13.5.

7. REFERENCES

1. Sana Rehman; Danish Ahmed. Embryology, Kidney, Bladder, and Ureter. Treasure Island (FL): StatPearls Publishing; 2020.
2. Sadler TW. Urogenital system. In: Taylor C, Pecarich L, editors. Langman's Medical Embryology. 13th ed. London: Wolters Kluwer; 2015. p. 250-3.
3. Mescher AL. The Urinary System. In: Lange, editor. Junqueira's Basic Histology. 14th ed. London: McGraw-Hill Education; 2016. p. 393-406.
4. Maslen CL, Babcock D, Redig JK, Kapeli K, Akkari YM, Olson SB. CRELD2: gene mapping, alternate splicing, and comparative genomic identification of the promoter region. Gene. 2006;382:111-20.
5. Oh-hashi K, Kunieda R, Hirata Y, Kiuchi K. Biosynthesis and secretion of mouse cysteine-rich with EGF-like domains 2. FEBS Lett. 2011;585:2481-7.
6. Park SJ, Kim Y, Chen YM. Endoplasmic reticulum stress and monogenic kidney diseases in precision nephrology. Pediatr Nephrol. 2019;34:1493-1500
7. Oh-hashi K, Koga H, Ikeda S, Shimada K, Hirata Y, Kiuchi K. CRELD2 is a novel endoplasmic reticulum stress-inducible gene. Biochem Biophys Res Commun. 2009;387:504-10.
8. National Center for Biotechnology Information (NCBI)[Internet]. Bethesda (MD): National Library of Medicine (US), National Center for Biotechnology Information; [2021] – [cited 2021 July 08]. Available from: https://www.ncbi.nlm.nih.gov/gene/79174
9. National Center for Biotechnology Information (NCBI)[Internet]. Bethesda (MD): National Library of Medicine (US), National Center for Biotechnology Information; [2021] – [cited 2021 July 08]. Available from: https://www.ncbi.nlm.nih.gov/gene/76737
10. Ortiz JA, Castillo M, del Toro ED, Mulet J, Gerber S, Valor LM et al. The cysteine-rich with EGF-like domains 2 (CRELD2) protein interacts with the large cytoplasmic domain of human neuronal nicotinic acetylcholine receptor alpha4 and beta2 subunits. J Neurochem. 2005;95:1585-96.
11. Oh-hashi K, Norisada J, Hirata Y, Kiuchi K. Characterization of the Role of MANF in Regulating the Secretion of CRELD2. Biol Pharm Bull. 2015;38:722-31
12. Oh-Hashi K, Fujimura K, Norisada J, Hirata Y. Expression analysis and functional characterization of the mouse cysteine-rich with EGF-like domains 2. Sci Rep. 2018;8:12236.

13. Kim Y, Park SJ, Manson SR, Molina CA, Kidd K, Thiessen-Philbrook H et al. Elevated urinary CRELD2 is associated with endoplasmic reticulum stress-mediated kidney disease. JCI Insight. 2017;2:e92896.
14. Li C, Chen YM. Endoplasmic reticulum-associated biomarkers for molecular phenotyping of rare kidney disease. Int J Mol Sci. 2021;22:2161.
15. Lin JH, Walter P, Yen TS. Endoplasmic reticulum stress in disease pathogenesis. Annu Rev Pathol. 2008;3:399-425.
16. Lasić V, Kosović I, Jurić M, Racetin A, Čurčić J, Šolić I. GREB1L, CRELD2 and ITGA10 expression in the human developmental and postnatal kidneys: an immunohistochemical study. Acta Histochem. 2021;123:151679.
17. Yamada Y, Arai T, Sugawara S, Okato A, Kato M, Kojima S et al. Impact of novel oncogenic pathways regulated by antitumor miR-451a in renal cell carcinoma. Cancer Sci. 2018;109:1239-53.
18. Kenter AT, van Rossum-Fikkert SE, Salih M, Verhagen PCMS, van Leenders GJLH, Demmers JAA et al. Identifying cystogenic paracrine signaling molecules in cyst fluid of patients with polycystic kidney disease. Am J Physiol Renal Physiol. 2019;316:F204-F213.
19. Wang Y, Shen J, Arenzana N, Tirasophon W, Kaufman RJ, Prywes R. Activation of ATF6 and an ATF6 DNA binding site by the endoplasmic reticulum stress response. J Biol Chem. 2000;275:27013-20.
20. Hong M, Luo S, Baumeister P, Huang JM, Gogia RK, Li M, Lee AS. Underglycosylation of ATF6 as a novel sensing mechanism for activation of the unfolded protein response. J Biol Chem. 2004;279:11354-63.
21. Shen J, Prywes R. ER stress signaling by regulated proteolysis of ATF6. Methods. 2005;35:382-9.
22. Shen J, Snapp EL, Lippincott-Schwartz J, Prywes R. Stable binding of ATF6 to BiP in the endoplasmic reticulum stress response. Mol Cell Biol. 2005;25(3):921-32.
23. Jao TM, Nangaku M, Wu CH, Sugahara M, Saito H, Maekawa H et al. ATF6α downregulation of PPARα promotes lipotoxicity-induced tubulointerstitial fibrosis. Kidney Int. 2019;95:577-89.
24. Boyle ST, Poltavets V, Kular J, Pyne NT, Sandow JJ, Lewis AC et al. Publisher Correction: ROCK-mediated selective activation of PERK signalling causes fibroblast reprogramming and tumour progression through a CRELD2-dependent mechanism. Nat Cell Biol. 2020;22:908.

25. Jariwala U, Prescott J, Jia L, Barski A, Pregizer S, Cogan JP et al. Identification of novel androgen receptor target genes in prostate cancer. Mol Cancer. 2007;6:39.
26. Dennis EP, Edwards SM, Jackson RM, Hartley CL, Tsompani D, Capulli M et al. CRELD2 is a novel LRP1 chaperone that regulates noncanonical WNT signaling in skeletal development. J Bone Miner Res. 2020;35:1452-69.
27. Wang Y, Zhou CJ, Liu Y. Wnt Signaling in Kidney Development and Disease. Prog Mol Biol Transl Sci. 2018;153:181-207.
28. Howell BW, Hawkes R, Soriano P, Cooper JA. Neuronal position in the developing brain is regulated by mouse disabled-1. Nature. 1997;389:733-7.
29. Sheldon M, Rice DS, D'Arcangelo G, Yoneshima H, Nakajima K, Mikoshiba K et al. Scrambler and yotari disrupt the disabled gene and produce a reeler-like phenotype in mice. Nature. 1997;389:730-3.
30. Gao Z, Godbout R. Reelin-Disabled-1 signaling in neuronal migration: splicing takes the stage. Cell Mol Life Sci. 2013;70:2319-29.
31. Arimitsu N, Mizukami Y, Shimizu J, Takai K, Suzuki T, Suzuki N. Defective Reelin/Dab1 signaling pathways associated with disturbed hippocampus development of homozygous yotari mice. Mol Cell Neurosci. 2021;112:103614.
32. Yoneshima H, Nagata E, Matsumoto M, Yamada M, Nakajima K, Miyata T et al. A novel neurological mutant mouse, yotari, which exhibits reeler-like phenotype but expresses CR-50 antigen/reelin. Neurosci Res. 1997;29:217-23.
33. Onoue A, Takeuchi M, Kohno T, Hattori M. Aberrant fragment of Dab1 protein is present in yotari mouse. Neurosci Res. 2014;88:23-7.
34. Bock HH, Herz J. Reelin activates SRC family tyrosine kinases in neurons. Curr Biol. 2003;13:18-26.
35. Rice DS, Sheldon M, D'Arcangelo G, Nakajima K, Goldowitz D, Curran T. Disabled-1 acts downstream of Reelin in a signaling pathway that controls laminar organization in the mammalian brain. Development. 1998;125:3719-29.
36. Yip YP, Kronstadt-O'Brien P, Capriotti C, Cooper JA, Yip JW. Migration of sympathetic preganglionic neurons in the spinal cord is regulated by Reelin-dependent Dab1 tyrosine phosphorylation and CrkL. J Comp Neurol. 2007;502:635-43.
37. Bock HH, May P. Canonical and Non-canonical Reelin Signaling. Front Cell Neurosci. 2016;10:166.

38. Racetin A, Jurić M, Filipović N, Šolić I, Kosović I, Glavina Durdov M et al. Expression and localization of DAB1 and Reelin during normal human kidney development. Croat Med J. 2019;60:521-31.
39. Racetin A, Filipović N, Lozić M, Ogata M, Gudelj Ensor L, Kelam N et al. A Homozygous Dab1-/- Is a Potential Novel Cause of Autosomal Recessive Congenital Anomalies of the Mice Kidney and Urinary Tract. Biomolecules. 2021;11:609.
40. Gao Z, Chen X, Zhu K, Zeng P, Ding G. Dab1 contributes to angiotensin II-induced apoptosis via p38 signaling pathway in podocytes. Biomed Res Int. 2017;2017:2484303.

8. SUMMARY

Objectives: The expression and localization of Creld2 in the nephrons of *yotari* (Dab1$^{-/-}$) and *wildtype* (Dab1$^{+/+}$) mice was analyzed to further develop its suggested importance in mammal kidneys overall, and its significance particularly in *yotari* mice nephrons.

Materials and methods: *Yotari* and *wildtype* mice were sacrificed on the 13.5th embryonal day, and the 4th and 14th postnatal day. Paraffin embedded kidney tissue sections were analyzed by immunofluorescence using Creld2 antibodies. Kidney structures were then examined by fluorescence microscope. The percentages of positive cells in the different nephron structures were compared between *yotari* and *wildtype* mice and analyzed by a Kruskal-Wallis test, followed by a t-test.

Results: The PCT of postnatal 14D *wildtype* nephrons showed a strong Creld2 expression signal in the cell cytoplasm and was the structure with the highest percentage of immunoreactive cells (95%) with significantly higher expressions compared to the *yotari* mice group ($P<0.05$). The PCTs of postnatal 4D *wildtype* kidney samples showed significantly higher Creld2 expressions compared to the *yotari* group ($P<0.05$). In both mouse groups, the PCTs of 14D postnatal kidneys showed a significantly higher Creld2 expression when compared to the 4D postnatal kidneys ($P<0.05$). In the E13.5 *yotari* and *wildtype* kidney samples, immunoreactive cells were exclusively detectable in the glomeruli, with the *wildtype* group showing significantly higher Creld2 expressions ($P<0.05$). The DCTs of both *yotari* and *wildtype* kidneys showed mild Creld2 expression with no significant differences found between the mouse groups.

Conclusions: Postnatally Creld2 was found to have a possible role in tubular function maintenance especially in the PCT and lesser in the DCT. The appearance of significantly high Creld2 expression in the *wildtype* glomeruli during the fetal kidney development confirm the potential significant role of Creld2 in the formation of kidney structure. Overall, *yotari* mice showed lower Creld2 expressions compared to the healthy controls, which might implicate a delayed kidney development in *yotari* mice.

9. CROATIAN SUMMARY

Naslov: PRIKAZ IZRAŽAJA CRELD2 U EMBRIONALNOM I POSTNATALNOM BUBREGU DAB1$^{-/-}$ MIŠA

Cilj: Analizirali smo izražaj i lokalizaciju Creld2 u nefronima *yotari* miševa (Dab1$^{-/-}$) i divljeg tipa (Dab1$^{+/+}$) kako bi se dalje utvrdio njegov predloženi značaj u bubrezima sisavaca općenito, kao i njegov značaj posebno u bubrezima *yotari* miševa.

Materijali i metode: *Yotari* miševi i miševi divljeg tipa žrtvovani su 13.5-og embrionalnog dana, te četvrtog i četrnaestog postnatalnog dana. Parafinski rezovi bubrežnog tkiva analizirani su imunofluorescencijom pomoću Creld2 protutijela. Bubrežne strukture ispitivane su fluorescencijskim mikroskopom. Postotak pozitivnih stanica između svake skupine uspoređen je i analiziran pomoću Kruskal-Wallis testa i potom korištenjem t-testa.

Rezultati: PCT 14 postnatalnih dana starog nefrona divljeg tipa pokazao je jaku ekspresiju Creld2 signala u staničnoj citoplazmi i bila je struktura sa najvećim postotkom imunoreaktivnih stanica (95%) sa signifikantno višom ekspresijom u usporedbi s grupom *yotari* miševa ($P<0,05$). PCT u 4 postnatalnih dana starom bubregu divljeg tipa pokazao je signifikantno veću Creld2 ekspresiju u usporedbi s *yotari* grupom ($P<0,05$). U obje grupe miševa, PCT u 14 postnatalnih dana starom bubregu pokazao je signifikantno veću ekspresiju Creld2 u usporedbi s 4 dana starim postnatalnim bubregom ($P<0,05$). U 13.5 dana embrionalnog razvoja starom bubrežnom uzorku *yotari* miša i miša divljeg tipa imunoreaktivne stanice su bile isključivo detektirane u glomerulu, gdje je grupa divljeg tipa pokazala signifikantno veću Creld2 ekspresiju ($P<0,05$). DCT u bubrezima *yotari* miša i miša divljeg tipa pokazao je slabu Creld2 ekspresiju bez nađene značajne razlike između mišjih grupa.

Zaključci: Postnatalno je Creld2 pronađen u mogućoj ulozi održavanja tubularne funkcije, posebno u PCT-u i nešto manjoj u DCT-u. Naizgled signifikantno velike Creld2 ekspresije u glomerulu divljeg tipa tijekom fetalnog razvoja bubrega potvrđuje potencijalnu signifikantnu ulogu Creld2 u formiranju bubrežnih struktura. Sveukupno, *yotari* miševi su pokazali nižu Creld2 ekspresiju u usporedbi sa zdravom skupinom, što ukazuje na zakašnjeli razvoj bubrega u *yotari* miševa.

10. CURRICULUM VITAE

Personal Data

Name and Surname:	Nikolina Đurđević
Date and place of birth:	07.12.1996 in Stuttgart, Germany
Citizenship:	German, Croatian
Address:	Vinodolska 21, 21000 Split, Croatia
E-mail:	n-durdevic@t-online.de

Education

October 2015 – July 2021	Studies of Human Medicine at the University of Split School of Medicine
2007 – 2015	Ferdinand-Porsche-Gymnasium Zuffenhausen, Stuttgart, Germany

Work experience

21/12/2020 – 14/03/2021	Internship at the Katharinenhospital (Klinikum Stuttgart), Germany Internal medicine (Oncology) Surgery (Traumatology, Pediatric surgery, General surgery)
01/08 – 01/09/2019	Clinical Traineeship Karl-Olga-Hospital Stuttgart, Germany Cardiology department

Other activities

Student representative of the sixth year at Medical School

Member of CroMSIC

Anatomy demonstrator

Languages

German – Native
Croatian – Native
English – C1
French – B2
Latin – Latinum